Journal of Alloys and Compounds 504S (2010) S467–S471

Contents lists available at ScienceDirect

Journal of Alloys and Compounds

journal homepage: www.elsevier.com/locate/jallcom

Molecular dynamics and first-principles studies on the deformation mechanisms of nanostructured cobalt

G.P. Zheng*

Department of Mechanical Engineering, The Hong Kong Polytechnic University, Hung Hom, Kowloon, Hong Kong

ARTICLE INFO

Article history:
Received 3 July 2009
Received in revised form
22 December 2009
Accepted 21 February 2010
Available online 4 March 2010

Keywords:
Nanostructured materials
Mechanical properties
Molecular dynamics simulations
Atomic scale structure

ABSTRACT

Deformation mechanisms of nanostructured cobalt are investigated by classical molecular dynamics (MD) simulation and first-principles calculation. In MD simulation, deformation twinning and HCP-to-FCC transformation are found to play important roles during the deformation of nanostructured cobalt. At high stress levels, the HCP-to-FCC transformation seems to overwhelm the deformation twinning. In particular, when deformation occurs in nanocrystalline cobalt with pre-existing twins, (0 0 0 1) twins are transformed into FCC structures through the deformation mechanism of HCP-to-FCC transformation. The generalized planar fault energy (GPFE) curves calculated by density functional theory are used to elucidate the deformation processes such as stacking faults, deformation twinning and HCP-to-FCC allotropic transformation observed in nanostructured cobalt. It is demonstrated by the GPFE curves that HCP-to-FCC transformation is more favorable than deformation twinning when hydrostatic pressures or shear stresses are applied on cobalt.

1. Introduction

Mechanical properties of nanocrystalline (nc) metals (with grain size less than 100 nm) can exhibit unusual behaviors compared with their coarse-grained counterparts. For example, the hardness and yield stress may increase five to ten times when the grain size is reduced from the macroscopic to the nanometer range. Several concrete deformation mechanisms such as grain boundary (GB) sliding, deformation-induced grain rotation, emission of partial dislocation from GB, deformation twinning and de-twinning have been proposed either from experiments [1] or from molecular dynamics (MD) simulations [2]. The deformation twinning and deformation de-twinning during the deformation of nc metals have attracted considerable attentions since such deformation mechanisms could provide us with methods to improve the ductility of those high-strength yet brittle nc metals. For example, pre-existing twins in nc face-centered cubic (FCC) copper [3] and aluminum [4] are found to contribute to the plasticity of these nc metals through the deformation de-twinning processes under high applied stresses.

Despite remarkable progresses on the investigation of the deformation mechanisms of nc metals, the precise nature of the deformation mechanism is still in considerable debate especially in those nc metals with non-FCC structures. Hexagonal close packed (HCP) metals such as Mg, Zn, Ti, Zr and Co are important industrial materials and the deformation mechanisms of HCP nc metals and alloys are of great interests. Recent experiments have shown that electrodeposited nc cobalt [5] and cobalt alloy [6] exhibit some unusual mechanical properties such as remarkable work hardening and ductility comparable to those of coarse-grained cobalt because of the high concentration of stacking faults (SFs), lamellar structures and micro-twins in these materials. The experimental results on cobalt and cobalt alloys suggest that the deformation mechanisms of HCP metals could be different with those in FCC nc metals.

In this study we investigate the deformation mechanisms of nc cobalt using classical MD simulation and first-principles calculations. In our previous MD studies [7,8] on nc cobalt with an average grain size of about 10 nm we found out some surprising results that although the stacking fault energy of cobalt is small, it is hard to observe the mechanical twinning during the plastic deformation process, even at high stress levels. In the contrast, we found that the deformation mechanism of nc cobalt is HCP-to-FCC transformation, which may result in remarkable plasticity in the nc cobalt. In this paper, we further elucidate the deformation induced structural transformation from different aspects as follows. First, we demonstrate in MD simulation that this deformation mechanism is general in nc cobalt with grain sizes larger than 10 nm. Second, the deformation mechanism is investigated in nc cobalt with pre-existing twins using MD simulation, which will reveal the competition between HCP-to-FCC transformation and deformation twinning processes. Third, density functional theory is used to calculate the energetics of HCP-to-FCC transformation and deformation twining in cobalt under different stress states that are common in nano-

* Fax: +852 23654703.
E-mail address: mmzheng@polyu.edu.hk.

0925-8388/$ – see front matter © 2010 Elsevier B.V. All rights reserved.
doi:10.1016/j.jallcom.2010.02.144

grains of nc metals because of the complicate structures of grain boundaries.

2. MD simulations of nanostructured cobalt and nc cobalt with pre-existing twins

2.1. MD simulation of cobalt with two-dimensional columnar structures

The columnar nc cobalt structure is shown in Fig. 1(a). The columnar direction (z-axis) is along [1 1 **2** 0] which is perpendicular to the Burgers vector $\mathbf{b}_p$ = 1/3 [**1** 1 0 0] in four identical columnar nanocrystals. The grain size is about 40 nm. The [**1** 1 0 0] directions of grains 1–4 form angles 21.87°, 43.74°, 65.6° and 109.35° to the x-direction respectively. Tensile stress is applied in the x-direction. Deformation in a constant stress mode is performed under the scheme of isostress–isoenthalpic ensemble at T = 300 K. Periodic boundary condition is used in each direction. A tight binding potential with second-moment approximation (Cleri–Rosato potential) [9] is used to describe the interaction among cobalt atoms. Fig. 1(c) and (d) shows the atomic structures in each nano-grain where the HCP atoms are in gold, FCC atoms are in pink, disordered atoms are in red and other 12-coordinated (non-FCC and non-HCP) atoms are in silver. When the strain is 3% or the stress is 3.2 GPa, the deformation twinning occurs by the passing of partials with Burgers vector $\mathbf{b}_p$ in each slip plane, which may result in the growth of the 1st grain. When the strain is increased to 8% or the stress is 5.8 GPa, the activities of deformation twinning are reduced since the partials tend to be emitted and travel on every second slip plane. The overlap of the SFs thus results in lamellar FCC structure. These results are consistent with our previous MD simulation [8] on nc cobalt with grain size of 8 nm, suggesting that the HCP-to-FCC allotropic transformation is a general phenomenon in nc cobalt under high applied stresses. The transformation is not through the nucleation of disordered clusters or FCC nuclei. Instead it can be considered as consequent passing of partials, similar to the deformation twinning, but on every second slip plane.

2.2. MD simulation of nc cobalt with pre-existing twins

The nc cobalt sample consisting of 23 grains is shown in Fig. 1(b). The GBs in this nc cobalt are typical high-angle ones, and the average grain size is 7.4 nm. There are 10% randomly distributed (0 0 0 1) twins (twin faults with . . .AB**ABC**BCB. . . stacking sequence) in each grain. The twin thickness is randomly chosen to be roughly 3–5 spacing of close-packed planes. The MD simulation method is the same as described in Section 2.1. Fig. 3 shows a grain with two pre-existing twins under various applied tensile stresses. When the applied stress is 5.6 GPa, a partial is emitted from the GB and on a slip plane adjacent to one of the twin boundary (TB), which results in the reduction of the twin thickness by one (0 0 0 1) atom layer (Fig. 2(b)). When the applied stress is 6.2 GPa, a full dislocation with a Burgers vector $\mathbf{b}$ = 1/3[**1** 2 **1** 0] nucleates inside the twinned region and splits into two partials through the reaction $\mathbf{b} \rightarrow 1/3[0\,1\,\mathbf{1}\,0] + \mathbf{b}_p$, as shown in Fig. 2(d). These two partials travel toward the GBs and the twinned region is transformed into lamellar FCC structure completely (Fig. 2(f)). The HCP-to-FCC transformation inside the twinned region can be attributed to the large shear stress near the TBs especially when deformation twinning occurs. These deformation behaviors further demonstrate that the HCP-to-FCC allotropic transformation is dominant deformation mechanism in nc cobalt under high applied stresses.

3. First-principles calculations of generalized planar fault energy of cobalt

As mentioned above, the deformation twinning and HCP-to-FCC transformation are all related to the slips of partial dislocations. The deformation twinning is caused by the passing of partials on each slip plane, whereas the HCP-to-FCC transformation can be consid-

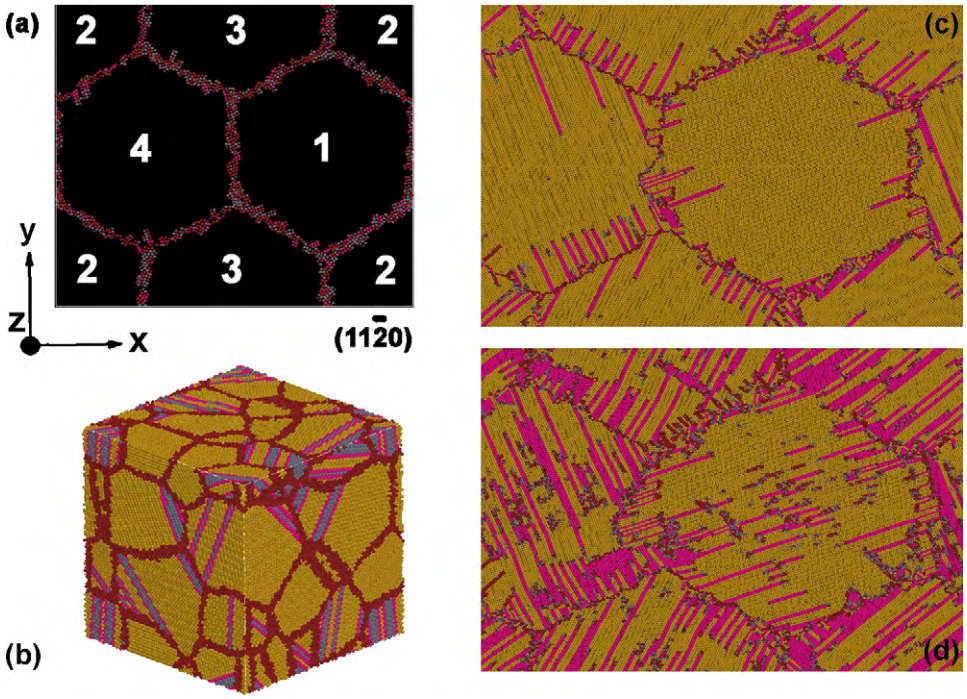

Fig. 1. (a) The textured columnar cobalt sample used for MD simulation. Only the non-HCP atoms are projected into the (1 1 **2** 0) plane (X–Y plane). The numbers are grain labels. (b) The nc-cobalt samples consisting of (0 0 0 1) twins. The grain boundary atoms are in red. The twinned region is in grey and HCP atoms are in yellow. The twin boundary atoms are in pink. (c and d) The columnar cobalt nanocrystals shown in (a) are deformed under 3% and 8% strains respectively. (For interpretation of the references to color in this figure legend, the reader is referred to the web version of the article.)

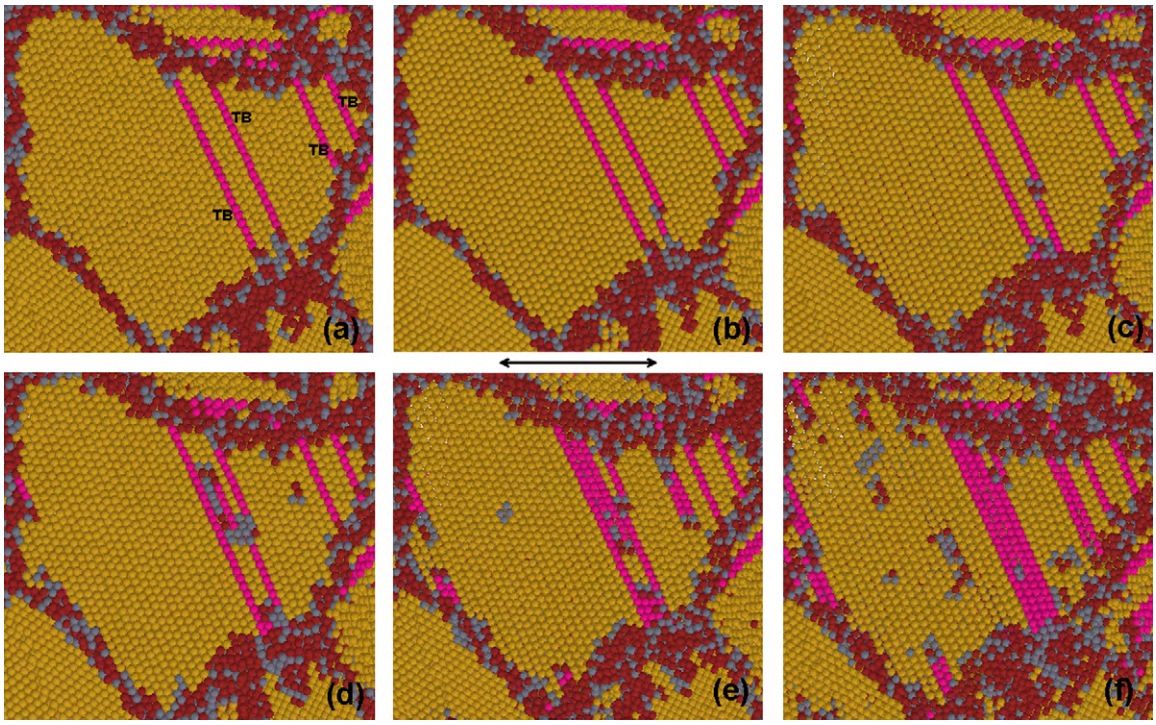

Fig. 2. The evolution of twin boundary (TB) and formation of lamellar FCC structures in nc cobalt sample with (0 0 0 1) pre-existing twins at strains: (a) 0%; (b) 6.2%; (c) 7.3%; (d) 8.7%; (e) 10.8%; (f) 14%. Atoms in the grain are projected on the (1 1 **2** 0) plane. The arrow in the middle indicates the direction of applied tensile stress.

ered as consequent passing of partials on every second slip plane. The generalized planar fault energy (GPFE) or the energetics of passing a leading partial, passing a trailing partial on the nearest neighbor slip plane or on the next nearest neighbor plane could provide us with important information on the deformation mechanisms. In this section we calculate the energetics of HCP-to-FCC transformation and deformation twining using density functional theory (DFT), which is necessary since it describes the free energy, phase diagram and magnetic properties of cobalt very well. Empirical potential (in Section 2) cannot describe the phase diagram and magnetic behaviors of cobalt successfully, resulting in subtle difference of GPFE if we use it to investigate cobalt under various stress states.

Calculations are performed using the VASP code [10] based on the spin-polarized density functional theory, which utilizes a plane-wave basis set for expansion of the single-particle Kohn–Sham wave functions and fully non-local Vanderbilt ultrasoft pseudopotential (US-PP) to describe the electron–ion interactions. For the Co pseudopotential the nonlinear core corrections are included, which are especially important for the description of the magnetic properties of Co. The exchange-correlation functional is approximated with Perdew–Wang 1991 version of the generalized gradient approximation, which employs the spin interpolation proposed by Vosko et al. [11]. The plane-wave cutoff energy is fixed at 480 eV throughout our calculations. A fictitious temperature for broadening of the electron states is set to 0.2 eV under Methfessel–Paxton scheme to improve the convergence. Brillouin zone *k*-point sampling is performed using the Monkhorst–Pack algorithm with $8 \times 12 \times 1$ grid centered at the Gamma point, which is adequate for good convergence.

The planar faults can be introduced by cutting a cobalt perfect supercell into two parts and shifting the upper part with respect to the lower part along a fault vector **f** on the fault plane (Fig. 3(a)). Three types of faults can be distinguished in Co, i.e. stacking fault, twin fault (TF) and FCC fault (FCCF). These faults give rise to different alterations of the stacking sequences of close-packed (0 0 0 1)

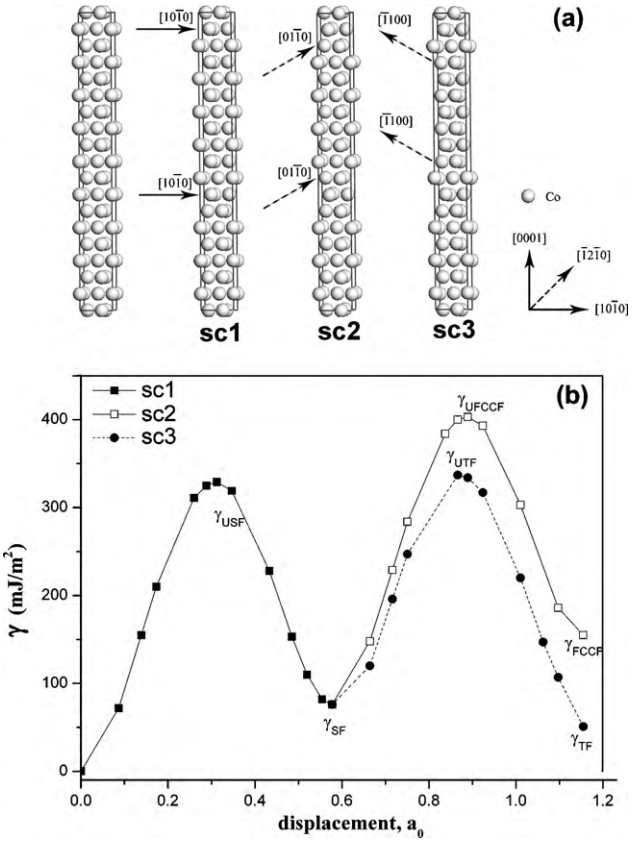

Fig. 3. (a) Co supercells used for the calculations of generalized planar fault energy. The arrows indicate the slip planes and slip directions. (b) The GPFE curves of cobalt calculated from density functional theory. The GPFE curves for twin fault and FCC fault are shifted by $a_0/3^{1/2}$ in the displacement axis. The legends denote the displacement directions and slip planes as indicated in (a).

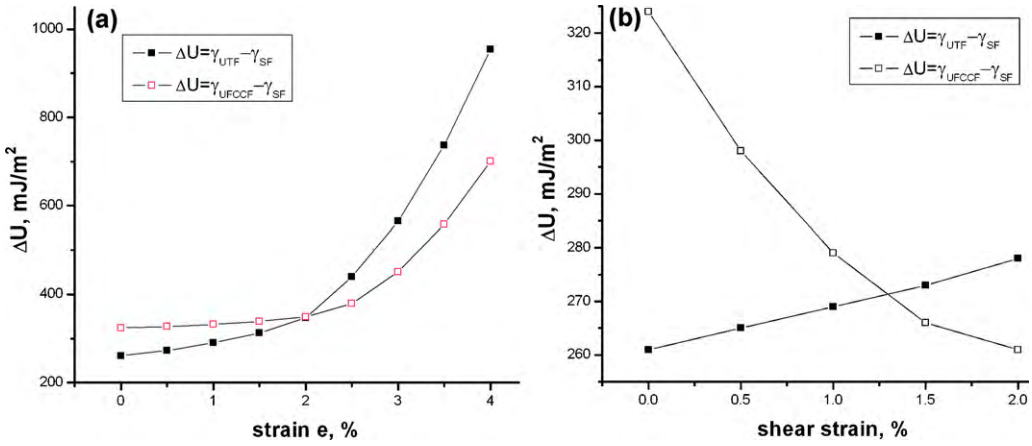

Fig. 4. (a) The energy barriers for the formation of twin fault (solid symbols) and FCC fault (opened symbols) under hydrostatic pressures. The compressive strain in each direction is *e*. (b) The energy barriers for the formation of twin fault and FCC fault under shear strains.

planes. In the case of a stacking fault, the starting configuration is a perfect supercell, and in the cases of twin fault and FCC fault the starting configurations are the supercells with pre-existing SF. The difference between forming a twin fault and a FCC fault is to proceed with the rigid slip in the nearest neighbor and next nearest neighbor planes of the faulted plane respectively.

The supercells used for first-principles calculations have orthorhombic structure, with lattice vectors aligned at the $[\bar{1}\,2\,\bar{1}\,0]$, $[1\,0\,\bar{1}\,0]$ and $[0\,0\,0\,1]$ crystallographic directions, and respective lengths of $a_0 = 0.2511$ nm, $\sqrt{3}a_0$ and $9c_0 = 3.654$ nm. In the $[0\,0\,0\,1]$ direction, there are totally eighteen atom layers and each layer contains two atoms. For each supercell (SC1 or SC2 or SC3) shown in Fig. 3(a) two structurally equivalent planar faults are introduced to make three-dimensional periodicity. In the undistorted HCP supercell, the stacking sequences are **BABABABABABABABA**. By displacing from the seventh to the eighteenth layers along the $[1\,0\,\bar{1}\,0]$ direction, two I2 intrinsic stacking faults (SC1 in Fig. 3(a)) are formed and the corresponding stacking sequences are **BABABABCACACACACAC**. Based on the stacking-fault supercell SC1, the shearing from the eighth to the seventeenth layers along the $[1\,\bar{1}\,0\,0]$ direction leads to the formation of twin faults (SC2 in Fig. 3(a)) with stacking sequences of **BABABABCBABABABABC**. Similarly, as to the formation of two FCC faults (SC3 in Fig. 3(a)), the tenth to the sixteenth layers of the stacking-fault supercell are displaced along the $[0\,\bar{1}\,1\,0]$ direction. The resulting stacking sequence now becomes **BABABABCABCBCBCBAC**. The interaction between the two planar faults can be neglected, since the faults are at least three layers (for FCC fault) apart.

The GPFE is calculated by the equation $\gamma(f) = [E(f) - E_0]/2S$, which represents a relation between planar fault energy γ and displacement f. Here $E(f)$ is the total energy of the supercell with planar faults, and E_0 is the total energy of a perfect HCP supercell. Before reaching three minimum energies in three GPFE curves as shown in Fig. 3(b), i.e. the SF energy (γ_{SF}), the twin fault energy (γ_{TF}) and the FCC fault energy (γ_{FCCF}), there are corresponding energy barriers to form the SF, twin fault and FCC fault, named as unstable stacking fault energy (γ_{USF}), unstable twin fault energy (γ_{UTF}) and unstable FCC fault energy (γ_{UFCCF}) respectively. These special values of energies are important parameters for the deformation of the materials and are illustrated in Fig. 3(b). At each small displacement, only the atom positions along $[0\,0\,0\,1]$ are allowed to relax until the total energy is converged to 1 meV.

In Fig. 3(b), we can find that the energy barrier $\Delta U = \gamma_{UFCCF} - \gamma_{SF}$ for the formation of FCC fault is larger than that ($\Delta U = \gamma_{UTF} - \gamma_{SF}$) for the formation of twin fault. These energy barriers will be significantly changed when stresses are applied on the supercells. Fig. 4(a) shows the changes of ΔU when hydrostatic pressures are applied on the supercells, and e measures the compressive strain caused by the pressure. When $e > 2\%$ or the pressure is larger than 7.5 GPa, ΔU for the formation of FCC fault is smaller than that for the formation of twin fault. The effects of shear stress on the competition between FCC fault and twin-fault formations are also investigated. Shear strain is applied to the supercell along $[\bar{1}\,2\,\bar{1}\,0]$ and the volume of the supercell is conserved during the shear. Fig. 4(b) shows the relations between the energy barriers and the shear strain. $\Delta U = \gamma_{UFCCF} - \gamma_{SF}$ for the formation of FCC fault significantly decreases with increasing shear strain and is lower than that for the formation of twin fault when the strain is larger than 1.6%.

The GPFE thus explains the deformation mechanisms observed in the MD simulations. At lower applied stresses, the energy barrier for deformation twinning is smaller than that for HCP-to-FCC transformation. When the applied stresses are high, cobalt tends to be deformed through HCP-to-FCC transformation since the energy barrier of forming the FCC faults is smaller than that of forming the twin fault. The competition between deformation twinning and HCP-to-FCC transformation during the plastic deformation process, characterized by the GPFE curves, thus offers an explicit atomistic picture in illustrating the different deformation mechanisms observed in experiments and MD simulations.

4. Conclusions

MD simulations are used to investigate the deformation of nc cobalt. It is found the HCP-to-FCC allotropic transformation is dominant deformation mechanism in nc cobalt under high applied stresses. We analyze the deformation mechanisms of nc cobalt using the concept of GPFE which characterizes the energetics of twin fault or HCP-to-FCC transformation. A systematic first-principles investigation is performed to calculate the GPFE curves of cobalt. It is found cobalt tends to be deformed through HCP-to-FCC transformation since the energy barrier for the formation of FCC faults becomes smaller than that for the formation of twin fault if the applied stresses are high. Hence the first-principles results explain the different deformation mechanisms observed in MD simulations on the deformation of nanostructured cobalt successfully.

Acknowledgments

Support from the Research Grants Council of the Hong Kong Special Administrative Region, China (Project No. PolyU 7200/05E) is acknowledged. The author is grateful for the supports provided

by the Research Funds of Hong Kong Polytechnic University (Project No. A-SA29).

References

[1] M. Chen, E. Ma, K.J. Hemker, Y.M. Wang, X. Cheng, Science 300 (2003) 1275.
[2] J. Schiotz, F.D. Di Tolla, K.W. Jacobsen, Nature 391 (1998) 561.
[3] L. Lu, X. Chen, X. Huang, K. Lu, Science 323 (2009) 607.
[4] H. Van Swygenhoven, P.M. Derlet, A.G. Froseth, Nat. Mater. 3 (2004) 399.
[5] A.A. Karimpoor, U. Erb, K.T. Aust, G. Palumbo, Scripta Mater. 49 (2003) 651.
[6] Y. Nakamoto, M. Yuasa, Y. Chen, H. Kusuda, M. Mabuchi, Scripta Mater. 49 (2003) 651.
[7] G.P. Zheng, Y.M. Wang, M. Li, Acta Mater. 53 (2005) 3893.
[8] G.P. Zheng, Acta Mater. 55 (2007) 149.
[9] F. Cleri, V. Rosato, Phys. Rev. B 48 (1993) 22.
[10] G. Kresse, J. Furthmüller, Phys. Rev. B 54 (1996) 11169.
[11] S.H. Vosko, L. Wilk, M. Nusair, Can. J. Phys. 58 (1980) 1200.